Acta Parasitologica
https://doi.org/10.1007/s11686-021-00387-3

ORIGINAL PAPER

Label-Free Quantitative Proteomic Analysis of Three Strains of Viscerotropic *Leishmania* Isolated from Patients with Different Epidemiological Types of Visceral Leishmaniasis in China

Fu-rong Wei[1] · Chun-hua Gao[1] · Jun-yun Wang[1] · Yue-tao Yang[1] · Feng Shi[1] · Bin Zheng[1]

Received: 29 January 2021 / Accepted: 29 March 2021
© Witold Stefański Institute of Parasitology, Polish Academy of Sciences 2021

Abstract

Background There are three epidemiological types of visceral leishmaniasis in China, which are caused by *Leishmania* strains belonging to the *L. donovani* complex. The mechanisms underlying their differences in the population affected, disease latency, and animal host, etc., remain unclear. We investigated the protein abundance differences among *Leishmania* strains isolated from three types of visceral leishmaniasis endemic areas in China.

Methods Promastigotes of the three *Leishmania* strains were cultured to the log phase and harvested. The protein tryptic digests were analyzed with liquid chromatography-electrospray ionization-tandem mass spectrometry (LC-ESI-MS/MS), followed by label-free quantitative analysis. The MS experiment was performed on a Q Exactive mass spectrometer. Raw spectra were quantitatively analyzed with the MaxQuant software (ver 1.3.0.5) and matched with the reference database. Differentially expressed proteins were analyzed using the bioinformatics method. The MS analysis was repeated three times for each sample.

Results A total of 5012 proteins were identified across the KS-2, JIASHI-5 and SC6 strains in at least 2 of the three samples replicate. Of them, 1758 were identified to be differentially expressed at least between 2 strains, including 349 with known names. These differentially expressed proteins with known names are involved in biological functions such as energy and lipid metabolic process, nucleotide acid metabolic process, amino acid metabolic process, response to stress, cell membrane/cytoskeleton, cell cycle and proliferation, biological adhesion and proteolysis, localization and transport, regulation of the biological process, and signal transduction.

Conclusion The differentially expressed proteins and their related biological functions may shed light on the pathogenicity of *Leishmania* and targets for the development of vaccines and medicines.

Keywords *Leishmania* · Visceral leishmaniasis · Proteomics · Label-free

Introduction

Visceral leishmaniasis (kala-azar) is a severe vector-borne parasitic disease of humans and other mammals caused by protozoan parasites *Leishmania donovani* complex leading to a significant health problem worldwide [1, 2]. The disease is endemic in 61 countries and is responsible for the annual loss of an estimated 1.81 million disability-adjusted life-years and 57,000 lives [3]. Out of the 20 neglected tropical diseases (NTDs) prioritized by the World Health Organization, the leishmaniases rank in the top 3 among those caused by protozoa [4].

Leishmania parasite uses vector sand flies for transmission and when they feed on an infected mammalian host, the amastigote forms are taken up by sand flies. Amastigote

✉ Jun-yun Wang
wangjy@nipd.chinacdc.cn

✉ Bin Zheng
zhengbin@nipd.chinacdc.cn

[1] National Institute of Parasitic Diseases, Chinese Center for Disease Control and Prevention (Chinese Center for Tropical Diseases Research), NHC Key Laboratory of Parasite and Vector Biology, WHO Collaborating Centre for Tropical Diseases, National Center for International Research on Tropical Diseases, Ministry of Health, Shanghai 200025, China

Published online: 21 May 2021

forms parasite differentiated into other stages, metacyclic promastigote present into the foregut of the vector sand and gets transferred to a new mammalian host when flies take another blood meal. A host plays a role as a reservoir host if it can transmit the parasite into the next stage that is into the vector [5]. *Leishmania* parasites are obligate intracellular pathogens that preferentially invade macrophages where they replicate, ultimately causing a heterogeneous group of diseases. The outcome of *Leishmania* infection depends on parasite virulence, and the genetic background and immune response of the host. While the clinical manifestation is determined by infecting parasites, the molecular mechanisms are elusive. The post-transcriptional and/or post-translational regulation of *Leishmania* genes involved in biological processes is important for the adaptation of parasites to the parasitophorous vacuole and to circumvent the immune responses of the host. Hence, proteome profiling of *Leishmania* promastigotes will help identify key molecules involved in these processes [6–8]. Quantitative proteomics is an important tool for analyzing the differential expression of proteins at different conditions. The label-free quantification is one such tool that relies on the separation of peptides from digested protein through liquid chromatography followed by the introduction of ionized peptides into a mass spectrometer [6–8].

In China, VL remains an important public health problem and is endemic or re-emerging in more than 50 counties in 6 provinces/autonomous regions in western China, including Xinjiang, Gansu, Sichuan, Shaanxi, Shanxi, and Inner Mongolia [9–12]. There are three epidemiological types of visceral leishmaniasis in China, based on the *Leishmania* species and the source of infection. Although they are all caused by *Leishmania* strains belonging to the *L. donovani* complex and present with similar clinical manifestations, there are differences in the population affected, the disease latency, and animal host, etc. Two epidemiological types of VL in China [13, 14], the anthroponotic type of VL (AVL), and the zoonotic type which is caused by *L. infantum* with an animal host as the principal source of infection. The zoonotic type has been further divided into two subtypes, a mountainous sub-type of zoonotic VL (MST-ZVL) and a desert sub-type of zoonotic VL (DST-ZVL), based on the ecosystem and epidemiological characteristics, i.e., geographical and landscape characteristics, age distribution of patients, vector sandfly species and their ecology, and source of infection. All of the three types are caused by *Leishmania* strains of the *L. donovani* complex, showing differences in the population affected, disease latency and animal host, etc., despite similar clinical manifestations [15].

To clarify the mechanisms underlying the differences, we conducted liquid chromatography-electrospray ionization tandem mass spectrometry on protein tryptic digests of promastigotes of three *Leishmania* strains isolated from three types of visceral leishmaniasis endemic areas in China, followed by label-free quantitative analysis. The present study aimed to analyze the protein abundance differences among *Leishmania* strains isolated from patients in three VL endemic areas using quantitative mass spectrometry. The study found the presence of 1758 proteins differentially abundant at least between 2 strains, of which 349 with names are involved in biological functions such as energy and lipid metabolic process, nucleotide acid metabolic process, amino acid metabolic process, response to stress, cell membrane/cytoskeleton, cell cycle and proliferation, biological adhesion and proteolysis, localization and transport, regulation of the biological process, and signal transduction.

Materials and Methods

Ethics Statement

The *leishmania* strains involved in this study were collected by the Institute of Parasitic Disease Prevention and Control, China Center for Disease Control and Prevention. The Institute for Parasitic Disease Prevention and Control of China Center for Disease Control and Prevention approved to use of the strains in this study. The patient information involved is anonymous.

Animal care and handling were following the standards specified in the Guidelines for the Care and Use of Laboratory Animals and approved by the Ethics Committee for Animal Care and Experimentation (SYXK 2016-0019) and international animal experimentation guidelines were followed. The study and its protocols were approved by the Ethics Committee of the National Institute of Parasitic Diseases, Chinese Center for Disease Control and Prevention. All surgeries were performed under sodium pentobarbital anesthesia and every effort was made to minimize the suffering of the animals.

Leishmania Strain Culture

Three *Leishmania* strains (Table 1) isolated from patients in different endemic areas in China were continuously passaged in golden hamsters to maintain virulence. Amastigotes were purified as previously described [16]. Amastigotes were isolated from spleens of the infected hamsters, cultured in the Novy-McNeal-Nicolle medium at 24 °C for 7 days, and then transferred to the 199 media with 10% heat-inactivated fetal calf serum for mass culture at 24 °C. Parasites were subcultured to inoculums of 2×10^6/mL, and amastigotes were harvested at the stationary phase, washed in sterile phosphate-buffered saline (PBS, pH: 7.2–7.4), and immediately used for protein extraction.

Table 1 Information of *Leishmania* strains

Strains	WHO code	Species	Location of isolation	Host	Epidemiological types of VL
KS-2	MHOM/CN/1996/KS-2	*L. donovani*	Kashgar, Xinjiang, China	Human	AVL
SC6	MHOM/CN/1986/SC6	*L. infantum*	Jiuzhaigou, Sichuan, China	Human	MST-ZVL
JIASHI-5	MHOM/CN/2008/JIASHI-5	*L. infantum*	Jiashi, Xinjiang, China	Human	DST-ZVL

AVL Anthroponotic type of VL, *MST-ZVL* Mountainous sub-type of zoonotic VL, *DST-ZVL* Desert sub-type of zoonotic VL

Species Identification and Molecular Confirmation

The genomic DNAs of Leishmania isolates were extracted from the cultured parasite and the ribosomal DNA internal transcribed spacer 1 (ITS-1) was PCR amplified using gene-specific primers as described in earlier literature [17]. The PCR products of amplified ITS-1 were sequenced and the obtained sequences from isolates were aligned with reference ITS-1 sequences of Leishmania deposited in GenBank using GENEDOC software.

Protein Extraction and Digestion

The amastigote pellets were suspended on ice in 200 µL lysis buffer (4% SDS, 100 mM DTT, 150 mM Tris–HCl pH 8.0) with agitation using a homogenizer (Fastprep-24®, MP Biomedical), and boiled for 5 min. The samples were further ultrasonicated, boiled for another 5 min, and centrifuged at 14 000 rpm for 15 min. The supernatant was collected and quantified with a BCA Protein Assay Kit (Bio-Rad, USA). Digestion of protein (250 µg for each sample) was performed according to the FASP procedure described by Wiśniewski et al. [18]. Briefly, the detergent DTT and other low-molecular-weight components were removed with 200 µl UA buffer (8 M Urea, 150 mM Tris–HCl pH 8.0) by repeated ultrafiltration (Microcon units, 30 kD) facilitated by centrifugation. Then 100 µl of 0.05 M iodoacetamide in UA buffer was added to block reduced cysteine residues and incubated for 20 min in darkness. The filter was washed with 100 µl UA buffer three times and then 100 µl 25 mM NH_4HCO_3 washedtwice. Finally, the protein suspension was digested with 3 µg of trypsin (Promega) in 40 µl of 25 mM NH_4HCO_3 overnight at 37 °C, and the resulting peptides were collected as a filtrate. The peptide content was estimated by UV light spectral density at 280 nm using an extinction coefficient of 1.1 of 0.1% (g/l) solution that was calculated based on the frequency of tryptophan and tyrosine in vertebrate proteins.

Liquid Chromatography-Electrospray Ionization-Tandem Mass Spectrometry

The peptides from each sample were desalted on a C18 Cartridge (Empore™ SPE Cartridges C18 (standard density), bed I.D. 7 mm, volume 3 ml; Sigma), then concentrated by vacuum centrifugation and reconstituted in 40 µl of 0.1% (*v*/*v*) trifluoroacetic acid. MS experiments were performed on a Q Exactive mass spectrometer coupled to an Easy LLC system (Proxeon Biosystems, now Thermo Fisher Scientific). Five micrograms of peptides were loaded onto the C18-reversed-phase column (Thermo Scientific Easy Column, 10 cm long, 75 µm inner diameter, 3 µm resin) in buffer A (2% acetonitrile and 0.1% formic acid) and separated with a linear gradient of buffer B (80% acetonitrile and 0.1% formic acid) at a flow rate of 250 nL/min controlled by IntelliFlow technology over 120 min. The following gradient was used: 0%-45% buffer B for 0–105 min, 45–100% buffer B for105–110 min, and 100% buffer B for110–120 min. The MS data were acquired using a data-dependent top ten method dynamically choosing the most abundant precursor ions from the survey scan (*m/z*300–1800) for HCD fragmentation. The target value was determined based on the predictive Automatic Gain Control (pAGC). Dynamic exclusion duration was 25 s. The survey scans were acquired at a resolution of 70,000 at *m/z* 200 and the resolution for HCD spectra was set to be 17,500 at *m/z* 200. The normalized collision energy was 30 eV. The under-fill ratio, which specifies the minimum percentage of the target value likely to be reached at a maximum fill time, was defined as 0.1%. The instrument was run with peptide recognition mode enabled. The MS experiments were repeated three times for each sample.

Proteomics Data Analysis

The MS data were analyzed using MaxQuant software version 1.3.0.5 [19]. The MS data were searched against the

uniprot_Leishmania_genus_50931_20160303. fasta database (50,931 total entries, downloaded 03/03/2016). An initial search was set at a precursor mass window of 6 ppm. The search followed an enzymatic cleavage rule of Trypsin/P and allowed maximal two missed cleavage sites and a mass tolerance of 20 ppm for fragment ions. Carbamidomethylation of cysteines was defined as a fixed modification, while protein N-terminal acetylation and methionine oxidation were defined as variable modifications for database searching. The cutoff of the global false discovery rate (FDR) for peptide and protein identification was set to be 0.01. Label-free quantification was carried out with MaxQuant as described previously [20]. Protein abundance was calculated based on the normalized spectral protein intensity (LFQ intensity). Three biological replicates (amastigotes from three independent mice infections) were performed with two technical runs for all three isolates. To neutralize the residual FBS proteins from the study, the digested tryptic peptides of FBS were analyzed by LC–MS/MS after OFF-GEL fractionation and also without fractionation. A total of 189 FBS proteins were identified (Table S1). Proteomes of Leishmania are likely to be contaminated by fetal calf serum which is a major contaminant in proteomic analysis, therefore, we develop a new set of peptides with the bovine UniProt sequences of these 189 proteins and designated it as the FBS database. The top 30 proteins with the highest PSM numbers accounted for ~95% of all residual FBS proteins, which were designated as major contaminants in the study and excluded from proteomic analysis of Leishmania.

Bioinformatics Analysis

The database files obtained by MaxQuant were analyzed by Perseus software (version 1.3.0.5), and Omicsbean (http://www.omicsbean.cn/) was used to analyze bioinformatics of significantly differentially abundant proteins [21].

Statistical Analysis

Only proteins that were identified consistently in all the three replicates to be differentially abundant at least between two strains were included in the data set. Proteins with a *t*-test *p* value <0.05, and meanwhile up-regulated (indicated by LFQ intensity ratio) by >2-folds or down-regulated by <0.5-fold were considered to be differentially abundant.

Results

Molecular Confirmation of Isolates

A single band of ITS-1 with the size of about 310 bp was amplified from all three Leishmania isolates. The sequence analysis identified that ITS-1 amplified from anthroponotic Anthroponotic type of VL (AVL) isolates strain KS-2 contained 316 bp with sequence identical to ITS-1 sequence from L. donovani reference strain MHOM/CN/1996/KS-2 without any mutation. The ITS-1 amplified from Mountainous sub-type of zoonotic VL (MST-ZVL) isolates SC6 was 313 bp without any sequence variation identical to MHOM/CN/1986/SC6. The ITS-1 amplified from Desert sub-type of zoonotic VL JIASHI-5 isolate were 310 bp without any sequence variation identical to MHOM/CN/2008/JIASHI-5. The MST-ZVL SC6 and DST-ZVL JIASHI-5 isolates were closely related to *L. infantum* isolate from Karamay, Xinjiang (KXG-Xu, KXG-Liu, and KXG-927). The *L. donovani* isolates AVL KS-2 was closely related to a cluster of *L. donovani* (Data not shown).

Characterization of the Proteome of the Three Chinese Strains of *Leishmania*

In this study, we applied the label-free quantitative proteomics coupled with the LC–MS/MS approach to characterize the proteomes of three strains of *Leishmania* KS-2, SC6, and JIASHI-5 isolated in China. Non-redundantly, there was a sum of 5012 proteins identified across the 3 strains (Table S2), including 3594 proteins in the JIASHI-5 strain (Table S3), 3682 proteins in the KS-2 strain (Table S4), and 3724 proteins in the SC6 strain (Table S5). Of them, 2304 proteins were identified in all of the three strains (Table S6, Fig. 1), while 194, 238 and 896 proteins were strain-specific for KS-2, SC6, and JIASHI-5, respectively (Fig. 1).

Of the 2304 proteins, 1758 were identified to be differentially abundant at least between 2 strains, including 349 with known names, 990 uncharacterized proteins, and 419 putative proteins (Table S7). The numbers of differential proteins between any two strains are shown in Table 2. Fifty-nine proteins were found to be differentially abundant among the 3 strains (Fig. 2), of which 47 were down-regulated and 12 up-regulated in the KS2 strain compared with the JS5 strain, 42 down-regulated and 17 up-regulated in the SC6 strain compared with the JS strain, and 33 down-regulated and

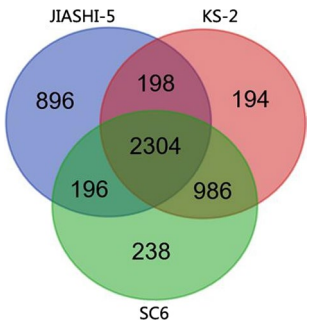

Fig. 1 Diagram of abundant proteins among the three strains

Table 2 Distribution of proteins differentially or uniquely expressed between any two strains

Comparisons	Number of differentially or uniquely expressed proteins	Number of up-regulated proteins	Number of down-regulated proteins
KS-2 *vs*JIASHI-5	1218	308	910
SC6 *vs*JIASHI-5	1219	341	878
SC6 *vs* KS-2	332	180	152

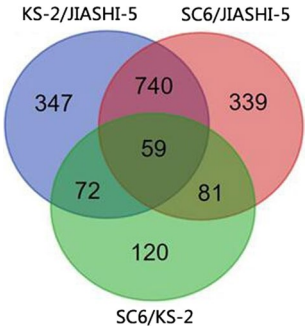

Fig. 2 Diagram of differentially abundant proteins between strains

26 up-regulated in the SC6 strain compared with the KS2 strain. In the study, 7.71% peptides spectra of Leishmania proteomes were derived from fetal calf serum considered to be false positives which were also confirmed by performing SILAC experiments to ensure they are having bovine origins for true identifications of peptides spectra of Leishmania proteomes.

Functional Annotation of the Identified Proteins

Gene ontologyanalysis was carried out to classify proteins based on biological processes. A majority of the proteins differentially abundant in all the three strains and the differentially abundant proteins with known names were involved in biological functions such as energy and lipid metabolic process, nucleotide acid metabolic process, amino acid metabolic process, response to stress, cell membrane/cytoskeleton, cell cycle and proliferation, biological adhesion and proteolysis, localization and transport, regulation of the biological process, and signal transduction. Based on protein annotation, the proteins differentially abundant in all the three strains were classified into the following functional categories directly associated with important biological processes: nucleotide acid metabolic process (13.06%); cellular protein biosynthetic process (9.42%); localization and transport (7.94%); enzyme metabolic process (5.21%); regulation of biological process (4.95%) and others (Fig. 3). The differentially abundant proteins with known names in the JIASHI-5 strain were mainly involved in the energy metabolic process (19.28%), nucleotide acid metabolic process (14.46%), amino acid metabolic process (8.41%), localization and transport (7.96%), cell membrane/cytoskeleton (5.22%) and response to stress (5.22%) (Table 3 and Fig. 4a). The differentially abundant proteins of the KS-2 strain were mainly involved in the energy metabolic process (19.91%), nucleotide acid metabolic process (12.83%), localization and transport (8.43%), amino acid metabolic process (7.63%), and response to stress (6.64%) (Table 3 and Fig. 3b). The differentially abundant proteins in the SC6 were mainly involved in the energy metabolic process (19.91%), nucleotide acid metabolic process (11.95%), localization and transport (8.41%), amino acid metabolic process (8.41%), and response to stress (6.19%) (Table 3 and Fig. 4c).

Fig. 3 Pie chart showing the relative distribution of proteins abundant in all the three *Leishmania* strains

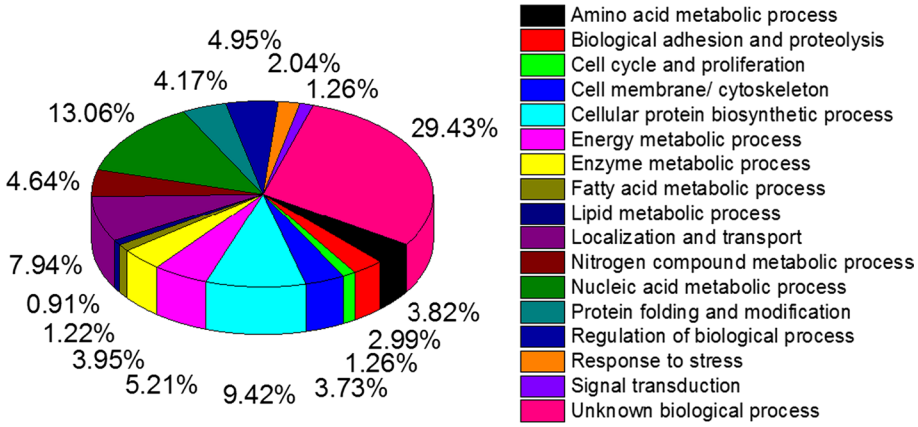

Table 3 List of the differentially expressed proteins with known names

Average LFQ intensity							
Protein name	Accession No	Matched peptides	Sequence coverage (%)	MW (kDa)	JIASHI-5	KS-2	SC6
Amino acid metabolic process							
Cysteine protease C	K4NQ58	12	37.7	37.491	6.37E+09	3.18E+09	3.73E+09
Aldehydedehydrogenase, mitochondrial	A4I1F4, Q25417, E9AXJ1	28	53.5	54.249	5.89E+09	4.49E+09	9.84E+09
Cysteine peptidase A (CBA)	E9BED5	9	23.2	38.902	2.09E+09	4.78E+08	6.44E+08
Proline oxidase, mitochondrial-like protein	A4I294	24	49.2	63.726	1.79E+09	4.14E+09	5.6E+09
Pyrroline-5-carboxylate reductase	E9BBL6	7	37.9	28.653	1.49E+09	2.09E+08	0
Arginase	A0A145YEM0	10	42.6	36.104	1.29E+09	2.62E+09	4.84E+09
Glutathione synthetase	A4HW34	14	34.2	67.082	1.14E+09	5.98E+08	3.48E+08
Acetylornithine deacetylase-like protein	A4HT45, Q4QIR7	13	37.3	43.052	1.03E+09	1.85E+09	3.39E+09
3-mercaptopyruvate sulfurtransferase	A4HSL9	12	42.4	40.241	5.45E+08	1.03E+09	4.36E+08
Cysteine protease b	M9SY92	8	24.3	48.07	4.39E+08	2.45E+08	1.94E+08
Pyridoxal phosphate containing glycine decarboxylase	A4I1U2	10	12.4	106.46	3.43E+08	6.23E+08	7.97E+08
Kynureninase	A4I2F1	6	18.4	50.696	3.04E+08	49,070,000	1.48E+08
Carboxypeptidase	A4HXS0	6	15.6	51.981	2.89E+08	40,430,000	64,451,000
Enoyl-CoA hydratase/isomerase-like protein	A4I4U5	6	29.2	29.036	1.9E+08	4.3E+08	2.57E+08
Cathepsin L-like cysteine protease (Fragment)	Q5EF91	2	8.9	24.368	82,921,000	26,997,000	0
Arginase (Fragment)	A0A145YEN9	4	9.4	36.012	55,941,333	3.75E+08	3.67E+08
Hydrolase-like protein	Q4QE87, A4HXI2	2	5.1	46.749	54,348,667	0	24,757,667
Glutamate dehydrogenase	Q4QF83	49	50.8	115.03	49,821,667	1.78E+09	5.73E+09
Monocarboxylate transporter-like protein	A4HSH0	2	3.7	61.634	0	0	1.13E+08
Cullin-like protein-like protein	Q4QAA1	3	4.7	85.44	0	30,008,000	24,126,667
Biological adhesion and proteolysis							
Proteasome subunit alpha type	A4HUT6, E9AVG6	12	47	27.818	2.29E+09	1.09E+09	1.57E+09
Pitrilysin-like metallo-protease	E9B921	19	23.9	115.44	9.23E+08	4.43E+08	3.67E+08
Proteasome subunit beta type	A4IBS2, A4IDD6	11	43.3	27.589	5.54E+08	1.6E+09	1.97E+09
GP63, leishmanolysin	A4HUG0, A4HUF6	14	23.5	81.516	5.01E+08	2.1E+08	65,887,667
Glycoprotein Gp63	Q94593	15	30.1	65.984	3.96E+08	5.63E+09	5.01E+09
Protoporphyrinogen oxidase-like protein	A0A0R6YBC7	2	11.3	25.223	65,992,667	50,986,667	0
Leishmanolysin	Q8MNZ1	14	27.7	70.342	0	2.24E+09	5.88E+09
Cell cycle and proliferation							
Guanine nucleotide-binding protein beta subunit-like protein	E9AH24, P62883	8	20.2	60.891	2.78E+08	32,873,667	21,414,667
Structural maintenance of chromosomes protein	A4IBP1, E9B9M1	10	9.2	146.97	1.75E+08	75,623,333	1.69E+08

Table 3 (continued)

Average LFQ intensity							
Protein name	Accession No	Matched peptides	Sequence coverage (%)	MW (kDa)	JIASHI-5	KS-2	SC6
Anaphase promoting complex, subunit 10-like protein	Q9TWN9	1	50	1.9102	1.73E+08	17,923,000	0
Autophagy-related protein	A4HYA5	2	15	16.602	1.47E+08	1E+08	69,045,667
MOB1 protein	A4H4Q9	3	13.7	29.026	1.01E+08	2.71E+08	2.48E+08
Serine hydroxymethyl-transferase	A0A088RV27	1	2.1	52.836	0	9,968,000	27,798,667
Cell membrane/cytoskeleton							
Tubulin beta chain	F8QV42	29	73.8	49.654	6.85E+09	3.1E+09	1.02E+10
Amastin	A5XDA6	5	28.4	19.578	3.02E+09	3.45E+09	7.97E+09
ADF/cofilin	A4I4A3	10	75.5	15.801	1.27E+09	76,466,667	0
Outer dynein arm docking complex protein	A4I8B1	19	34	70.369	9.56E+08	4.01E+08	9.16E+08
Intraflagellar transport protein-like protein	E9AH05	19	42.7	61.397	9.02E+08	2.65E+08	4.75E+08
Flagellar protofilament ribbon protein-like protein	A4HUN1	15	40.6	47.02	8.36E+08	3.3E+08	4.88E+08
Nucleolar protein family a member-like protein	A4IAG9	6	52.7	16.632	7.09E+08	1.86E+08	4.73E+08
Eukaryotic translation initiation factor 6	A4ICP5	8	51.4	27.084	5.5E+08	1.1E+09	1.41E+09
Tubulin binding cofactor A-like protein	A4I8B9	5	47.2	14.034	5.44E+08	1.51E+08	47,896,333
V-type proton ATPase proteolipid subunit	A4I051, A0A088RUF3	1	9	17.001	72,906,667	80,870,333	2.49E+08
Alpha tubulin (fragment)	Q66VD0	19	79.9	27.892	69,011,667	1.35E+09	4.37E+08
Alpha-tubulin *N*-acetyl-transferase	A4I1F7	3	15	27.135	19,996,333	0	0
Beta-tubulin	A4HLD6	12	63.3	20.507	14,256,333	2.79E+08	1.43E+09
Glycosomal membrane like protein	Q4QAW6, E9AH26, Q4Q839	5	26.4	23.68	0	1.15E+08	2.85E+08
Cellular protein biosynthetic process							
Oligosaccharyl transferase-like protein	A4IB08	12	18.1	96.093	9.82E+08	2.25E+09	3.78E+09
C-8 sterol isomerase-like protein	A4I4S3	3	14.8	24.915	5.73E+08	2.29E+08	3.97E+08
Tyrosyl or methionyl-tRNA synthetase-like protein	A4HX10	8	38	25.24	5.11E+08	1.71E+08	2.07E+08
Ubiquitin-activating enzyme-like protein	A4HTH3	5	8.1	113.78	96,221,000	0	90,200,000
Lipoate-protein ligase-like	A4HTD2	1	4.2	35.837	47,063,000	0	0
Frataxin-like protein	A4I1E7	2	13.8	20.296	40,754,333	0	0
Elongation factor-1 (Fragment)	Q25224	6	46.7	10.059	0	41,590,333	1.04E+08
Methylthioribose-1-phosphate i somerase	Q4Q0R9	8	23.7	40.418	0	2.51E+08	76,267,667

Table 3 (continued)

Average LFQ intensity							
Protein name	Accession No	Matched peptides	Sequence coverage (%)	MW (kDa)	JIASHI-5	KS-2	SC6
Elongation initiation factor 2 alpha subunit (fragment)	D9IDN3	16	58.8	28.493	0	3.94E+08	8.2E+08
Energy metabolic process							
Enolase	A4HW62, Q3HL75	28	75.1	46.036	2.24E+10	3.82E+10	5.4E+10
Cytochrome c oxidase subunit IV	E9AGF4	26	68.8	39.596	8.25E+09	4.49E+09	1.1E+10
Phosphomannomutase	A4IDG8	14	51.8	28.142	7.93E+09	4.28E+09	3.42E+09
Fumarate hydratase	A2CIN0	34	63.7	62.622	7.93E+09	2.59E+09	3.75E+09
Dipeptylcarboxypeptidase	A4HRR9	30	58	76.576	7.47E+09	3.55E+09	3.04E+09
Succinyl-CoA:3-ketoacid-coenzyme A transferase	E9AHQ2	21	49.9	52.629	4.24E+09	9.17E+09	1.3E+10
3-hydroxyisobutyryl-CoA hydrolase, mitochondrial	A4I8I5	14	46.3	39.61	3.22E+09	3.73E+08	1.42E+08
Succinate dehydrogenase (ubiquinone) flavoprotein subunit, mitochondrial	E9AH70	28	57.2	66.74	3.2E+09	5.31E+09	6.92E+09
ATP-binding cassette protein subfamily C, member 2	A4I060	35	29.8	172.24	2.5E+09	9.74E+08	4.6E+08
Glycerol-3-phosphate dehydrogenase [NAD(+)]	A4HUG3	7	24	39.259	1.73E+09	6.41E+08	1.3E+09
Isocitrate dehydrogenase (NADP)	A2CIA0	39	83.4	48.474	1.73E+09	2.86E+08	4.66E+08
6-phosphogluconate dehydrogenase, decarboxylating	Q18L02	16	47.4	51.944	1.23E+09	1.31E+08	4,852,667
ATPase ASNA1 homolog	A4HUY0	12	44.7	43.982	1.19E+09	5.33E+08	3.91E+08
UDP-glucose pyrophosphorylase	A4HXX2	11	31.4	54.364	1E+09	5E+08	6.84E+08
ATP binding protein-like protein	A4I8C0	8	43.9	22.199	7.03E+08	1.35E+08	1.24E+08
Ribokinase	A4I2M8	11	38	35.398	6.43E+08	2.28E+09	2.79E+09
ATP-binding cassette protein subfamily F, member 3	A4I8P8	10	20.7	74.736	6.27E+08	3.87E+08	2.74E+08
P27 protein	A4I3H5	8	37.9	27.633	6.25E+08	4.04E+08	9.29E+08
Dihydroorotate dehydrogenase	E9AGN2	7	24.6	33.894	5.48E+08	1.17E+09	8.31E+08
Pteridine reductase 1	A4I067	10	45.5	30.222	5.3E+08	1.16E+08	0
Glyceraldehyde-3-phosphate dehydrogenase-like protein	A4IC12	5	26.4	36.216	5.06E+08	1.64E+08	2.85E+08
Riboflavin kinase/fmn adenylyltransferase-like protein	A4IBK7, E9AFE0	3	19.1	20.531	4.74E+08	4.61E+08	1.57E+08
Glucosamine-6-phosphate isomerase	Q4Q4U6	7	34.8	31.524	4.47E+08	1.33E+08	3.33E+08
NADH-cytochrome b5 reductase	Q4QFH9, A4H9T1	11	49.1	31.512	4.21E+08	6.84E+08	1.39E+09

Table 3 (continued)

Average LFQ intensity							
Protein name	Accession No	Matched peptides	Sequence coverage (%)	MW (kDa)	JIASHI-5	KS-2	SC6
ATP-binding cassette protein subfamily F, member 1	A4HRS7	13	22.1	82.341	4.11E+08	1.71E+08	2.98E+08
Cytochrome c oxidase subunit I	Q4Q052	3	28.8	13.865	3.61E+08	4.36E+08	1.26E+09
Nuclear receptor binding factor-like protein	A4HSH5, Q4QJF0	7	24.7	35.776	3.27E+08	39,374,333	0
Citrate synthase	E9ARK6	11	23.8	52.26	2.67E+08	4.92E+09	5.68E+09
Tyrosine aminotransferase	E9BTV8	9	26.8	49.687	2.65E+08	4.38E+08	57,944,667
Phosphoacetylglucosamine mutase-like protein	E9B984	11	22.6	65.395	2.63E+08	1.18E+08	1.14E+08
Phosphatidic acid phosphatase protein-like protein	E9BEC7	5	19	44.533	2.4E+08	0	0
Membrane-bound acid phosphatase 2	Q4QB35	4	11.6	59.818	2.33E+08	0	48,806,667
Zinc binding dehydrogenase-like protein	A4HUG8, A4HUG9	3	12.4	39.527	2.24E+08	65,714,667	51,777,333
Receptor-type adenylate cyclase a-like protein	E9BU42	6	5.7	151.17	1.9E+08	93,050,000	55,121,000
Triosephosphate isomerase	A4I0S4	14	72.5	27.193	1.9E+08	15,417,000	52,910,333
NADH:ubiquinone oxidoreductase 78 Kd subunit-like protein	A4HY18	4	26.4	28.612	1.2E+08	0	0
ATP-binding cassette protein subfamily A, member 10	A4I4B4	4	3	206.97	95,645,000	2.19E+08	73,601,000
Mannose-6-phosphate isomerase	A2CIJ7	11	28.7	46.436	89,536,667	1.63E+08	3.02E+08
ATP-binding cassette protein subfamily H, member 2	A4I4M8	5	13.8	49.79	83,670,000	0	0
Methylmalonyl-coa epimerase-like protein	Q4Q9I9	2	14.2	15.347	78,126,667	0	0
LP7	A3EYC3	1	7.5	15.572	70,077,667	0	0
Glyceraldehyde-3-phosphate dehydrogenase	E9AT12	10	34.1	35.506	65,518,333	3.03E+08	2.06E+08
6-phosphogluconolactonase	A0A088RVT0	3	13.9	28.64	51,894,000	0	0
6-phosphofructo-2-kinase-like protein	A4HTA2	3	2.6	139.3	49,707,000	0	0
Quinone oxidoreductase-like protein	A4I0D8	4	18.8	36.616	42,319,000	1.22E+08	1.44E+08
Mannosyltransferase-like protein	Q4Q675	2	3.1	107.29	25,145,667	0	0
Glycosyl hydrolase-like protein	E9BPH8	2	1.7	152.03	14,217,000	0	0

Table 3 (continued)

Average LFQ intensity							
Protein name	Accession No	Matched peptides	Sequence coverage (%)	MW (kDa)	JIASHI-5	KS-2	SC6
5-Methyltetrahydropteroyltriglutamate-homocysteine *S*-methyltransferase	Q4Q6R3	31	38.3	86.109	9,977,333	4.45E+09	1.38E+09
Dehydrogenase-like protein	E9AXI1, A4HUB6	2	6.3	45.705	0	0	58,063,000
ATP-binding cassette protein subfamily G, member 6	A4ID77	1	1.5	74.487	0	12,188,033	5,533,567
Haloacid dehalogenase-like hydrolase-like protein	E9BJM0	2	4.2	44.484	0	16,399,000	39,108,333
Ribulose-phosphate 3-epimerase	A4I928	1	3	28.275	0	37,716,333	53,259,000
Malate dehydrogenase	E9B4I0	1	2.3	36.292	0	37,907,000	50,709,333
Carnitine palmitoyltransferase-like protein	Q4QBW4	3	6.7	74.777	0	69,954,000	75,695,000
Membrane-bound acid phosphatase	E9AT34	3	5.4	57.456	0	1.02E+08	75,910,667
Glycosomal glyceraldehyde 3-phosphate dehydrogenase (fragment)	A0A0R6HXP6	13	64.8	20.802	0	1.36E+09	5.07E+08
Transaldolase	A4HWX3	16	50.9	36.972	4.5E+09	1.79E+09	1.67E+09
S-adenosylmethionine synthase	E9AHK3	24	59.4	43.125	1.71E+09	81,936,667	27,566,667
Diphosphomevalonate decarboxylase	A4HXM8	12	37.1	42.405	6.43E+08	1.37E+09	1.32E+09
3-hydroxy-3-methylglutaryl coenzyme A reductase	A4I602	12	34.8	45.861	3.57E+08	6.64E+08	8.84E+08
Acetyl-coenzyme A synthetase	A0A088RTC5, A4I0C2	4	6.2	78.522	95,412,333	3.78E+08	8.05E+08
Galactokinase-like protein	A0A088S0U3, A4IBE2	8	18.9	53.271	75,926,333	39,606,667	1.49E+08
Fatty acid transporter protein-like protein	E9AH85	2	2.7	144.14	34,620,000	0	10,654,333
2,4-dienoyl-coa reductase-like protein	A4HSY5	2	4.1	80.432	19,797,667	0	0
Enzyme metabolic process							
Transaldolase	A4HWX3	16	50.9	36.972	4.5E+09	1.79E+09	1.67E+09
S-adenosylmethionine synthase	E9AHK3	24	59.4	43.125	1.71E+09	81,936,667	27,566,667
Diphosphomevalonate decarboxylase	A4HXM8	12	37.1	42.405	6.43E+08	1.37E+09	1.32E+09
3-hydroxy-3-methylglutaryl coenzyme A reductase	A4I602	12	34.8	45.861	3.57E+08	6.64E+08	8.84E+08
Acetyl-coenzyme A synthetase	A0A088RTC5, A4I0C2	4	6.2	78.522	95,412,333	3.78E+08	8.05E+08
Galactokinase-like protein	A0A088S0U3, A4IBE2	8	18.9	53.271	75,926,333	39,606,667	1.49E+08
Fatty acid transporter protein-like protein	E9AH85	2	2.7	144.14	34,620,000	0	10,654,333

Table 3 (continued)

Average LFQ intensity							
Protein name	Accession No	Matched peptides	Sequence coverage (%)	MW (kDa)	JIASHI-5	KS-2	SC6
2,4-dienoyl-coa reductase-like protein	A4HSY5	2	4.1	80.432	19,797,667	0	0
Fatty acid metabolic process							
Elongation of fatty acids protein	A4HSN8, A4I7T3, A4HW10, E9APR0, E9APR0, E9AGL0, E9B2P1	1	4	29.001	2.34E+08	0	18,846,667
Thiolase protein-like protein	Q4Q698, E9B1W4	17	36.8	46.891	1.73E+08	3.04E+08	6.16E+08
Lathosterol oxidase-like protein	A4I0I8	3	10.3	35.517	97,681,333	1.99E+08	2.64E+08
Lipoyl synthase, mitochondrial	E9ARY7	1	4.1	46.216	5,619,667	0	17,123,667
Lipid metabolic process							
4-coumarate:coa ligase-like protein	A4HYB7	25	43.1	66.105	2.05E+09	2.02E+09	4.19E+09
D-lactate dehydrogenase-like protein	E9BJC4	18	42.8	53.778	1.14E+09	4.01E+09	4.25E+09
Actin interacting protein-like protein	A4I0D2	14	34.1	56.947	6.67E+08	1.96E+09	1.46E+09
Mevalonate kinase	Q4Q6K7	10	41	35.484	6.33E+08	1.43E+09	1.22E+09
Inositol-3-phosphate synthase	Q4QFJ8	14	27.4	58.3	5.24E+08	1.49E+08	2.84E+08
Dihydroxyacetonephosphate acyltransferase	A4I9R9	9	7.1	154.57	1.22E+08	35,776,000	1.05E+08
Phosphoglycan beta 1,3 galactosyltransferase	A4HRS1	4	5.8	95.804	62,967,333	0	0
Phosphatidate cytidylyltransferase	E9AHM2	2	5.7	53.201	0	38,985,667	88,436,667
Glycerol-3-phosphate dehydrogenase	Q4Q8P6	11	20.7	66.533	0	1.45E+08	2.01E+08
Localization and transport							
Glucose transporter, lmgt2	A4IC74, Q4Q0D1	11	19	61.197	4.08E+09	6.53E+08	1.71E+09
Ubiquinol-cytochrome-c reductase-like protein	A4I763	6	47.1	7.9252	2.34E+09	8.38E+08	1.23E+09
Adenine aminohydrolase	E9AHV7	12	34.8	40.844	1.54E+09	4.18E+08	4.43E+08
Hydrophilic acylated surface protein a	A4I0F2	3	22.5	8.5447	8.26E+08	1.57E+08	0
Prefoldin subunit 4	A4I1C4	9	55.1	14.827	8.07E+08	1.36E+08	55,403,333
COP-coated vesicle membrane protein gp25L	A4IB85	6	31.8	24.332	7.79E+08	2.19E+08	1.6E+08
Amastin-like surface protein-like protein	A4I5B9, Q4QAK4	3	17.1	24.466	5.89E+08	87,186,667	46,966,667
Importin subunit alpha	A4I5E3	12	29.7	58.059	5.28E+08	1.34E+09	1.42E+09
Conserved SNF-7-like protein	A4IAV5	4	18.3	25.503	4.65E+08	1.09E+08	1.29E+08
Aldose 1-epimerase-like protein	A4I082, Q4QBD1	8	28.2	44.332	4.58E+08	2.19E+08	2.49E+08
COP-coated vesicle membrane protein erv25	A4IDI9	3	11.6	30.064	3.7E+08	1.85E+08	3.63E+08

Table 3 (continued)

Average LFQ intensity							
Protein name	Accession No	Matched peptides	Sequence coverage (%)	MW (kDa)	JIASHI-5	KS-2	SC6
MGT2 magnesium transporter	A4I1F1	6	15	46.019	2.61E+08	89,708,667	1.05E+08
Trypanin-like protein	A4IB81	7	22.1	54.077	2.61E+08	0	1.29E+08
Transportin2-like protein	Q4Q1E8	8	10.6	102.28	2.58E+08	5.52E+08	2.17E+08
Sre-2/carboxylate carrier-like protein	A4HSJ0	5	22.5	37.906	1.61E+08	4.08E+08	5.34E+08
Kinetoplast-associated protein-like protein	E9AD01, A4HU01, A4H5R1	3	91.9	78.801	1.6E+08	3.05E+09	1.64E+09
Lipophosphoglycan biosynthetic protein (Lpg2)	A4IA88	2	7	37.181	1.32E+08	0	0
Adaptin-related protein-like protein	A4HV08	5	4.6	108.42	69,718,000	0	0
SNF7-like protein	A0A088S2K6	1	6.5	24.672	53,466,000	0	0
AP complex subunit beta	A4ICB7	5	7.6	82.421	49,127,333	0	0
Derlin	A4I975	1	4.7	24.799	13,981,000	0	12,458,900
Phospholipid-transporting ATPase	Q4QG01	1	0.9	124.27	0	13,285,333	8,074,667
AP-3 complex subunit delta	A4HTF9	3	3.4	124.36	0	35,840,667	28,011,000
Iron/zinc transporter protein-like protein	Q4Q5V0	2	3.9	45.81	0	3.08E+08	3.77E+08
Nitrogen compound metabolic process							
60S acidic ribosomal protein P2	O43940	5	69.5	10.446	1.25E+10	4.69E+09	6.32E+09
40S ribosomal protein S19-like protein	A4I4Y2	8	57.8	18.104	6.86E+09	1.41E+10	7.36E+09
40S ribosomal protein S25	Q9N9V4	7	52.5	13.046	2.84E+09	1.17E+10	1.12E+10
60S ribosomal protein L37	P62885	4	32.5	9.8354	1.95E+09	1.16E+09	8.46E+08
60S ribosomal protein L32	A4HZH8	10	50.4	15.368	1.81E+09	7.76E+09	5.02E+09
40S ribosomal protein S12	A4HVI6	12	83.7	15.592	7.01E+08	93,954,667	12,925,333
50S ribosomal protein L13-like protein	A4IAD5	3	17.3	24.075	43,406,333	0	0
60S acidic ribosomal protein P2-2	Q06382	5	77.5	10.998	0	3.61E+08	8.13E+08
Nucleic acid metabolic process							
Histone H4	A0A0R4J969	9	53	11.422	3.18E+10	7.64E+09	4.73E+09
Nascent polypeptide-associated complex subunit beta	A4ID19	9	65	11.636	9.88E+09	4.76E+09	2.93E+09
Splicing factor ptsr1-like protein	A4HTB3	17	42.1	42.149	8.02E+09	3.33E+09	3.88E+09
Adenylosuccinate synthetase	A7LBL2	27	48.7	78.387	3.6E+09	8.26E+09	6.34E+09
Macrophage migration inhibitory factor-like protein	A4I971, A0A0R6YB83	5	68.1	12.72	2.49E+09	6.05E+08	2.55E+08

Table 3 (continued)

Protein name	Accession No	Matched peptides	Sequence coverage (%)	MW (kDa)	Average LFQ intensity JIASHI-5	KS-2	SC6
Ribonucleoside-diphosphate reductase	A4I3G6	24	37.2	90.964	1.72E+09	2.4E+09	8.52E+08
Nucleoside hydrolase-like protein (fragment)	Q2PD43	11	51	38.79	1.44E+09	5.89E+08	5.39E+08
Prefoldin 5-like protein	A4HZU4	8	72.6	17.9	1.26E+09	3.43E+08	2.95E+08
Myosin	B9UX70	25	31	119.18	1.09E+09	3.37E+08	4.43E+08
Obg-like ATPase 1	A4I330	15	49.5	44.019	1E+09	9.78E+08	4.92E+08
Nonspecific nucleoside hydrolasewith	E9BDY8	5	22.6	34.238	6.48E+08	1.32E+09	1.53E+09
Aminopeptidase-like protein	E9AHB1	11	16.5	98.014	4.64E+08	3.3E+08	1.23E+08
Xanthine phosphoribosyltransferase	E9AGU7	9	48.1	26.997	4.64E+08	2.92E+08	2.01E+08
DNA tovpoisomerase 2	E9BJW5	17	13.7	168.47	4.4E+08	35,875,000	1.96E+08
Alanine–tRNA ligase	Q4QBJ3	32	41.5	106.32	2.57E+08	1.01E+09	1.04E+09
Nucleoside phosphorylase-like protein	A4HUL2	8	26.7	36.877	2.25E+08	8.12E+08	6.9E+08
Dihydrofolate reductase-thymidylate synthase	E9AKW4, Q8MXB7	11	20.2	58.525	1.7E+08	1.3E+08	77,280,333
S-adenosylmethionine decarboxylase proenzyme	Q4Q6X9	4	15.2	43.087	1.34E+08	3.53E+08	1.91E+08
DNA topoisomerase I-like protein	Q8WQM6	4	24.8	28.162	1.34E+08	1.43E+08	0
Topoisomerase-related function protein-like protein	E9B969	4	7.3	99.694	1.26E+08	0	0
DNA topoisomerase	E9AZZ7	9	11.8	96.258	99,728,333	2.39E+08	3.12E+08
Adenosine kinase-like protein	A4IAC6	2	10.8	41.891	69,477,000	0	0
ATP-dependent RNA helicase-like protein	Q4Q0X4	5	8.3	106.78	68,424,667	56,318,333	0
DNA-directed RNA polymerase ii	E9ACT0	2	35.7	9.7553	43,545,333	0	0
DNA-directed RNA polymerase subunit beta	A4I1A3, E9AUE0	5	4.3	181.58	42,714,000	66,472,000	65,629,667
p1/s1 nuclease	A4I5I0, Q4Q7F3	1	3.8	35.016	42,385,000	0	0
Nucleoside hydrolase-like protein	E9BBP8	11	50.6	39.139	39,165,333	1.78E+08	2.2E+08
KRR1 small subunit processome component	A4I5Y2	2	6.5	36.07	36,288,667	0	0
REL1	Q6T451	2	4.5	54.17	33,069,000	10,823,000	0
DNA polymerase	A0A088S646	2	1.4	151.74	32,367,667	0	0
Dnaj chaperone-like protein	A4I8V3	2	6.2	63.203	28,749,000	0	0
Phosphoadenosine phosphosulfate reductase-like protein	A4I3B1	1	4.7	24.787	22,579,667	0	0
DNAj-like protein	E9B0N2, A4HYV5	1	2.6	46.997	13,665,667	0	3,966,333
DNA helicase	A4I9B0, A4I0T0	2	3.2	95.127	13,076,667	0	0
Peptide chain release factor-like protein	A0A088RSQ8	1	4.1	49.136	13,028,333	0	0

Table 3 (continued)

Average LFQ intensity							
Protein name	Accession No	Matched peptides	Sequence coverage (%)	MW (kDa)	JIASHI-5	KS-2	SC6
DNAJ protein-like protein	A4ICS3	1	5.8	27.776	12,281,333	0	0
Flap endonuclease 1	Q4FYU7	2	4.8	44.339	0	16,954,667	10,349,333
Nucleobase transporter	A4HUW2	1	2	59.801	0	24,470,333	1.92E+08
Nucleosome assembly protein-like protein	Q4Q687	11	33.8	45.379	0	24,645,000	81,111,333
RNasePH-like protein	E9AUS5	1	3.2	42.486	0	44,213,667	58,958,000
Protein SEY1 homolog	E9B2F8	3	3.7	97.928	0	71,403,333	85,254,000
Protein folding and modification							
Peptidyl-prolyl cis–trans isomerase	A0A088SFM4	3	12.2	24.573	1.86E+08	4.18E+08	3.29E+08
Serine/threonine-protein phosphatase	E9B9T9, E9AHT0, A0A088RP33, E9AGF3, A4I8C8	3	6	70.766	44,726,000	43,717,333	0
N-acetylglucosamine-6-phosphate deacetylase-like protein	A4ICY4	1	3	46.784	10,553,000	0	0
Sulfhydryl oxidase	Q4QF88	2	9	34.615	0	0	21,106,000
Peptidyl-prolyl cis–trans isomerase	E9AW05, A4IDA1, E9B9B2, A4I4Z7	7	25.5	31.389	0	78,528,333	2.26E+08
Regulation of biological process							
Protein disulfide-isomerase	E9BV84, A4ICD5	25	57.2	52.357	1.08E+10	4.45E+09	6.93E+09
Mitochondrial RNA-binding protein RBP38	Q86PT0	12	50.1	39.953	1.53E+09	8.95E+08	4.14E+08
Mitochondrial RNA binding protein 2	A4HU34	10	42.1	26.964	8.9E+08	1.86E+09	1.45E+09
Sideroflexin	A4HRI0	13	44.2	36.089	8.29E+08	1.83E+09	2.53E+09
Acetoin dehydrogenase e3 component-like protein	E9BN42	12	27.5	59.7	4.48E+08	1.11E+08	58,663,000
Glutaredoxin-like protein	A4HRD2	5	36.4	21.253	2.83E+08	38,076,333	0
Prohibitin	A4HX59	15	53.7	30.23	1.96E+08	1.06E+08	42,047,333
Inhibitor of cysteine peptidase	E9AH84, Q868G9	3	27.4	13.094	1.8E+08	2.36E+08	3.88E+08
Cyclin-dependent kinases regulatory subunit	A0A088RYR5	3	24.2	11.8	1.65E+08	5,318,000	0
Transcription activator	A4I966	6	6.9	125.94	45,721,667	0	0
Transcription factor-like protein	E9AGY6	7	11.9	84.706	35,329,667	1.68E+08	98,079,667
Oxidoreductase-like protein	A4I3H1, A4I0B8, E9AW62	2	2.2	107.47	30,153,667	2.66E+08	0
Farnesyltransferase beta subunit	A4I281	2	2.6	78.308	0	0	55,757,667
Contig, possible fusion of chromosomes 20 and 34	A4HAT2	1	2.5	47.646	0	52,994,000	24,013,333
Histone-lysine *N*-methyltransferase, H3 lysine-79 specific	A4I974	2	7.9	28.358	0	78,547,667	48,121,000
Response to stress							
Superoxide dismutase	A4I7Z7	6	37.9	21.527	2.47E+10	4.82E+09	2.26E+09
Cyclophilin 40	A4IC14	13	39.5	38.514	4.39E+09	1.36E+09	1.46E+09

Table 3 (continued)

Protein name	Accession No	Matched peptides	Sequence coverage (%)	MW (kDa)	Average LFQ intensity JIASHI-5	KS-2	SC6
Peroxidoxin 2	Q07DU5	17	77.9	22.222	1.99E+10	3.81E+10	4.35E+10
Tryparedoxin	E9BKS1, E9ADX4	8	57.2	16.697	1.32E+10	5.46E+08	71,349,333
Tryparedoxin peroxidase	E9BCF2, A4HWK2	16	74.9	22.179	3.48E+09	5.41E+08	2.94E+08
Peroxidoxin	E9BG25, Q95U89	17	73.9	25.384	1.47E+09	1.31E+08	45,454,333
Cystathionine beta-lyase-like protein	A4HVY9	11	29.3	56.713	4.32E+08	3.93E+08	1.36E+08
SURF1-like protein	Q4QGE3	9	32.1	40.286	3.19E+08	6.48E+08	6.71E+08
Cytosolic tryparedoxin	A5JV96, A8I4U5	9	57.2	16.67	2.26E+08	5.01E+09	5E+09
Peroxidoxin 1	Q07DU7	16	77.4	21.291	1.81E+08	30,722,667	0
p-glycoprotein e	A4I6Q3	11	9.3	183.83	1.62E+08	1.09E+08	29,555,000
Thioredoxin	E9AC16	3	30.8	12.015	1.17E+08	86,905,333	1.06E+08
Ecotin-like protein 2	Q4QFD4	4	25.9	17.846	1.1E+08	5.16E+08	3.45E+08
Heat shock protein 83–1	E9AHM8	49	60.9	78.785	15,388,667	3.13E+09	2.92E+09
Pentamidine resistance protein 1	A0A088RXT4	1	0.7	194.59	0	1.79E+08	1.03E+08
Chaperonin HSP60, mitochondrial	Q4Q1M0, E9ASX7	35	69.6	59.317	0	2.58E+08	5.75E+08
Signal transduction							
ADP-ribosylation factor-like protein 1	A4HX72	3	21.4	20.849	1.16E+08	2.4E+08	49,916,667
Mitogen-activated protein kinase	A4ICA4	5	16.8	41.067	1.05E+08	2.34E+08	0
Phosphodiesterase	Q4QF31, A4HWN7	24	27.7	103.8	77,648,667	3.79E+08	3.03E+08
ADP-ribosylation factor-like protein	Q4Q1Z4	2	12.3	32.758	71,095,333	32,466,333	0
Unknown biological process							
Stress-induced protein sti1	A4HTP4	45	64.3	62.239	1.37E+10	7.15E+09	5.91E+09
Reticulon-like protein	E9BM00	6	26.4	22.112	6.11E+09	2.32E+09	2.71E+09
18 kDa nuclear protein	Q8T9R3	2	19.8	11.162	4.58E+09	81,540,667	13,035,000
H1 histone-like protein	A4I9G5	2	33.1	14.11	3.48E+09	67,150,000	0
Small glutamine-rich tetratricopeptide repeat protein	A4I5V1	22	52.2	45.814	3.24E+09	1.04E+09	8.7E+08
Calmodulin-like protein	A4IBS7	9	69.8	15.708	1.69E+09	8.23E+08	1.2E+09
Ankyrin/TPR repeat protein	E9AH25	19	41.1	43.002	1.14E+09	2.4E+09	2.52E+09
Transmembrane 9 superfamily member	A4IAD3, E9BKX1	10	20.9	70.764	7.86E+08	2.91E+08	3.31E+08
Histone H2B	A4HY42, A4HXJ9	7	46.7	14.83	7.8E+08	5,951,667	10,801,567
Ghistone H1 like	E9AHF9	1	15.8	5.7819	6.61E+08	0	1.02E+08
RNA binding protein	A4HY39	11	47.2	42.522	6.28E+08	4.2E+08	2.78E+08
Paraflagellar rod protein-like protein	A4I2Z1	16	28.5	88.624	4.27E+08	1.82E+08	2.42E+08
Formate–tetrahydrofolate ligase	A4I5T5	19	35.7	66.63	3.09E+08	2.96E+09	2.12E+09
Na/H antiporter-like protein	E9BGB9	11	9.5	165.8	2.95E+08	1.82E+08	1.44E+08
Sulfurtransferase	A4HU69	4	55.5	13.037	2.37E+08	5.61E+08	6.43E+08
ORF10	Q25302	5	34.5	19.744	2.33E+08	44,723,000	16,360,000

Table 3 (continued)

Protein name	Accession No	Matched peptides	Sequence coverage (%)	MW (kDa)	Average LFQ intensity		
					JIASHI-5	KS-2	SC6
Similarity to endo-1-like protein	A4ICB3	1	7.5	26.413	1.96E+08	0	46,704,000
Programmed cell death 6 protein-like protein	A4HVS3	3	28.2	25.891	1.13E+08	0	0
Ubiquitin-fold modifier-conjugating enzyme 1	A4HWL0	2	19.3	19.456	1.1E+08	0	0
Golgi apparatus membrane protein TVP23 homolog	A4I2Z7	1	11.4	26.591	96,796,667	0	0
Peroxin 19	A4IBL7	3	18.4	33.784	78,773,333	0	0
Developmentally regulated phosphoprotein-like protein	A4HYM0	3	9.7	50.759	77,472,667	12,629,667	0
Homoserine dehydrogenase	A4HT44	5	16.7	39.968	63,146,333	0	20,329,000
ORF13	Q27681	5	6.8	94.538	57,945,000	1.11E+08	52,860,333
Beta-fructosidase-like protein	A4I0D9	2	4.5	62.232	52,890,000	20,376,333	0
Surface antigen-like protein	A4HS16, E9ACQ0	1	5.9	29.492	45,880,000	0	0
Cyclin-e binding protein 1-like protein	A4ICG6	3	5.1	74.824	45,069,000	0	28,110,667
3-Mercaptopyruvate sulfurtransferase	Q7JMY8	1	75	1.7288	44,346,667	0	1.08E+08
Periodic tryptophan protein 2-like protein	A4HXV7	1	1.5	102.89	42,605,667	0	29,371,667
Sec14, cytosolic factor	A4ICS6	2	5.4	48.513	41,546,667	0	24,748,667
Ferredoxin 2fe-2 s-like protein	A0A088RXU5	1	11.2	17.407	32,752,333	0	8,265,667
HSP70-like protein	A4HRI7	2	3	117.16	31,113,667	0	0
Phosphatidylethanolaminen-methyltransferase-lik e protein	A4I735, Q4Q632	1	5.5	23.32	22,610,000	0	0
Serine acetyltransferase	A4IA64	1	2.7	45.088	20,754,000	0	0
Defective in cullin neddylation protein	A4IAJ8	2	8.5	26.273	20,722,333	0	0
Aquaporin-like protein	A4I858	2	2.7	62.752	18,121,333	0	0
A44l protein-like protein	A0A088S510	1	1.5	81.348	16,534,667	0	0
Methyltransferase-like protein	A4IA51	1	2.1	46.717	0	20,696,667	11,497,333
Homoserine dehydrogenase-like protein	Q4QIR8	1	5.5	39.985	0	32,941,333	28,185,667
Kinesin-like protein (Fragment)	Q8WQZ1	1	14.5	16.542	0	41,909,000	34,647,000
Lysine decarboxylase-like protein	A0A088RMQ2	3	9	35.442	0	66,345,000	21,802,667
Viscerotropic leishmaniasis antigen	Q25416	3	26	59.573	0	79,520,667	86,700,000
Miltefosine transporter beta subunit	Q0P0L8	2	4.4	40.478	0	1.13E+08	1.36E+08
Copine i-like protein	Q4Q8E7	4	8.3	55.898	0	1.48E+08	1.25E+08

MW molecular weight

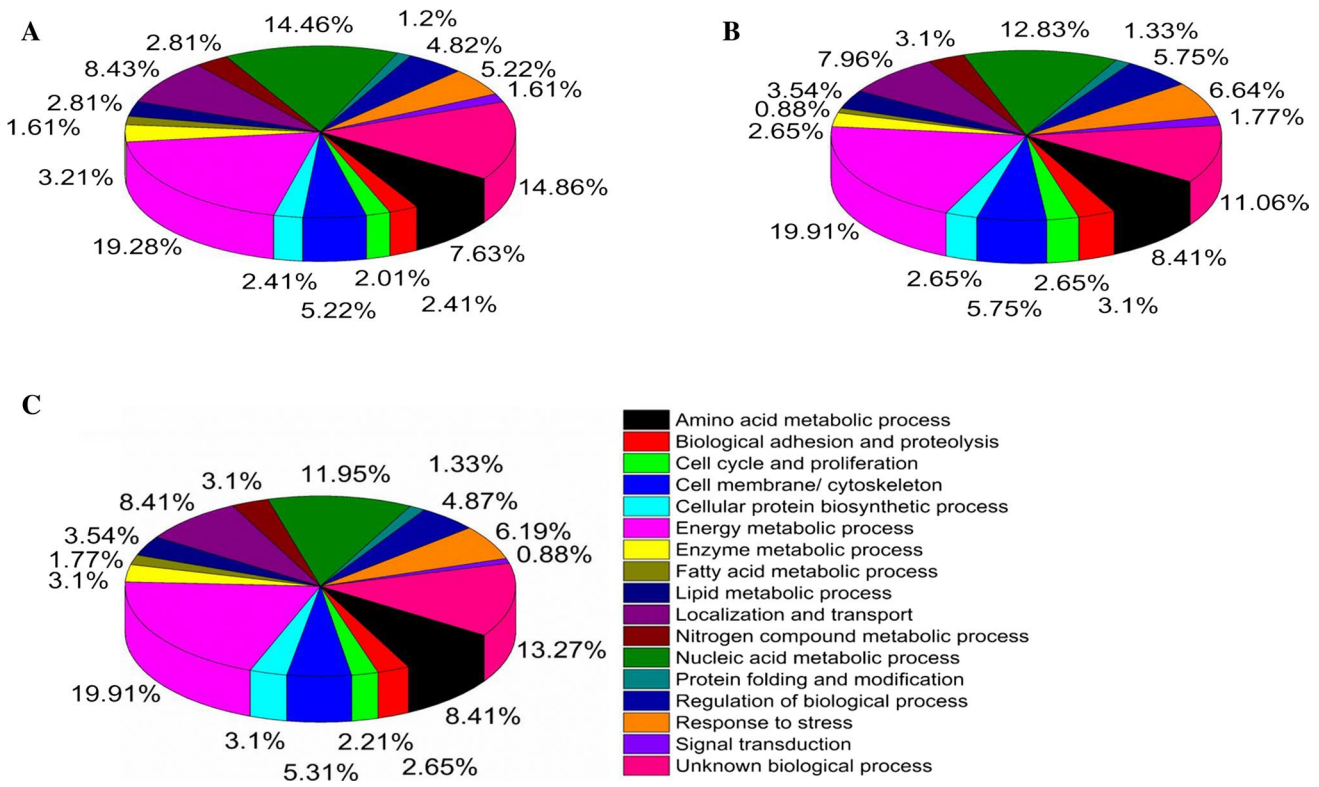

Fig. 4 Pie chart showing the relative distribution of differentially abundant proteins in *Leishmania* JIASHI-5 (**a**), KS-2 (**b**), and SC6 (**c**) strains

Discussion

In this study, we analyzed the protein abundance differences among three *Leishmania* strains (JIASHI-5, KS-2, and SC6) isolated from patients with VL in different epidemiological areas of China using the comparative proteomics method. A total of 5012 proteins were identified across all 3 *Leishmania* strains, and 1758 of them were differentially abundant (LFQ intensity ratio >2.0 or <0.5, $p<0.05$). The 349 differentially abundant proteins with known names were involved in biological functions such as energy and lipid metabolic process, nucleotide acid metabolic process, amino acid metabolic process, response to stress, cell membrane/cytoskeleton, cell cycle and proliferation, biological adhesion and proteolysis, localization and transport, regulation of the biological process, and signal transduction. Some of them have been associated with the virulence of several *Leishmania* species. The disease-causing capacity of *Leishmania* is linked to a complex interplay between the parasitic stress response, cell cycle regulation, and its differentiation into various life cycle stages that are adapted for survival and proliferation in the sandfly insect vector and mammalian host [22].

Cells that are more invasive and have a high rate of replication are expected with increased energy consumption and protein synthesis. Consistently, we observed S-adenosylmethionine decarboxylase (AdoMetDc), phosphomannomutase, NAD(P)H cytochrome b 5 oxidoreductase (Ncb5or), 6-phosphogluconate dehydrogenase (6PGDH), acetyl-CoA synthetase (AceCS) and elongation factor 2 (EF-2) indicate amplified precursor synthesis. Polyamines are small ubiquitous basic molecules that play multiple essential roles in cell development and proliferation in all classes of organisms. The polyamine biosynthesis pathway is essential for the viability, growth, and infectious mammalian stage of the trypanosomatid parasite including *Leishmania*, suggesting potential drug targets. AdoMetDc is a key enzyme of this pathway [23]. The importance of the polyamine biosynthesis pathway is demonstrated by the fact that AdoMetDc knockout in mice is lethal at early embryonic stages [24]. The S-adenosylmethionine decarboxylase proenzyme was more abundant in the KS-2 strain, and phosphomannomutase was highly abundant in JIASHI-5. The phosphomannomutase catalyzes the transformation of mannose-6-phosphate into mannose-1-phosphate, an important step in mannose activation and glycoconjugate biosynthesis in eukaryotes. The phosphomannomutase-deficient *L. mexicana* loses its virulence capability, suggesting that it can be used as a target for anti-Leishmanial inhibitors [25]. Ncb5or comprising cytochrome b 5 and cytochrome b 5 reductase domains(NADH-cytochrome b5 reductase was up-regulated in SC6 strain in this study.) is widely

distributed in eukaryotic organisms. The findings suggest that the decreased linoleate synthesis and increased oxidative stress and apoptosis are major consequences of *L. major* Ncb5or deficiency in *Leishmania* [26]. 6PGDH, which was up-regulated in theJIASHI-5 strain, is a key enzyme for oxidation in the generation of NADPH and ribulose 5-phosphate. This suggests that 6PGDH can be a potential target for the development of new therapeutic drugs against these parasites [27]. AceCS, which was up-regulated in the SC6 strain, is an enzyme of the acetate metabolic pathway. Other studies have demonstrated that *L. donovani* AceCS is important for *in vitro* macrophage infection and is essential for the biosynthesis of total lipids and ergosterol [28]. EF-2 is associated with the translation and elongation of polypeptide chains at ribosomes and has been associated with the virulence phenotype of *L. donovani* [29]. It is proposed that there are interactions between EF-2 and ribosomal structural subunits such as the 60S subunit of the L30 and 40S subunit of the S16 ribosomal protein, both of which are associated with translation [30].

Parasites have also developed resistance mechanisms to evade sandfly digestive enzymes and innate immune responses of the host, such as the mammalian complement system and macrophage defense mechanisms involving nitric oxide (NO). NO is produced by nitric oxide synthase 2(NOS2) from L-arginine. Arginase, which was up-regulated in the SC6 strain, is an immune-regulatory enzyme that reduces NO production from activated macrophages, limiting the availability of L-arginine to NOS2, thus supporting *Leishmania* resistance to the host defense mechanisms [31]. Glyceraldehyde 3-phosphate dehydrogenase (GAPDH) was up-regulated in the KS-2 strain, suggesting that changes in the expression of GAPDH may be responsible, at least in part, for the natural resistance to nitric oxide (NO) found in human and canine *Leishmania* spp. [32]. Cysteine protease (CP) was up-regulated in the JS5 strain. which are known to have an important role in the survival of the intracellular form of *L. donovani* [33].

Leishmania is auxotrophic for purines, and consequently, purine acquisition from the host is a requisite nutritional function for the parasite. Each genus of parasite has evolved a unique complement of purine salvage enzymes that enables it to scavenge host purines. *Leishmania* expresses several purine salvage enzymes, including hypoxanthine–guanine phosphoribosyltransferase (HGPRT), adenine phosphoribosyltransferase (APRT), xanthine phosphoribosyltransferase (XPRT) (highly abundant in the JIASHI-5), and adenosine kinase (AK) (JIASHI-5-unique) [34]. Purine interconversion enzymes are also expressed in *Leishmania*, most of which have human counterparts. Here, we found that adenine aminohydrolase and adenylosuccinate synthetase (ADSS) were up-regulated in the JIASHI-5 and KS-2 strains, respectively. The adenine aminohydrolase is a unique interconversion enzyme in purine salvage that converts 6-aminopurines into 6-oxypurines [35], while ADSS has been identified as vital components of purine salvage in *L.donovani*. ADSS deficiency has been shown to affect growth and cause infectivity phenotypes of *L. donovani* [36]. The protein p27 (Ldp27), which was up-regulated in the SC6 strain, is the component of an active cytochrome c oxidase complex in *L. donovani,* and deletion of its gene results in reduced virulence *in vivo* [37]. In another study, Ldp27$^{-/-}$ parasites did not survive beyond 20 weeks in BALB/c mice, suggesting that they can be used as a safe immunogen [38].

During *Leishmania* invasion, the infected macrophages activate a series of cytotoxic pathways in an attempt to kill the pathogen. These pathways include induction of NO biosynthesis and the release of radical oxygen species [39]. As a response, *Leishmania* parasites increase the secretion of certain proteins that protect against the stress response, such as tryparedoxin peroxidase and peroxidoxin. In addition, the tryparedoxin peroxidase, peroxidoxin, glutathione synthetase (GSS), thioredoxin (TRX) and superoxide dismutase were up-regulated, while cytosolic tryparedoxin was down-regulated in the JIASHI-5 strain. These proteins are associated with the *Leishmania* virulence phenotype [40–44]. A recent study shows that siRNA silencing of GSS and TRX enhances the leishmanicidal activity of glucantime [44]. Castro et al. [45] reported that interactions between tryparedoxin peroxidase and peroxidoxin, which has cellular detoxification functions and is involved in signaling, proliferation, and differentiation, are crucial for parasite survival in oxidative environments. Consistently, a comparative proteomic analysis of antimony-susceptible and antimony-resistant *L. braziliensis* and *L. chagasi*lines have shown up-regulated tryparedoxin peroxidase and peroxiredoxin in the resistant lines, suggesting that increased metabolism of peroxides and higher antioxidant defense play a significant role in the resistance of parasites to antimonials [46].

The increased survival could also be related to the increase of chaperones. HSP-70 (highly expressed in the JIASHI-5) is more abundant in cells that are stressed by elevated temperatures, protects proteins that have been denatured by heat as well as nascent peptides, and blocks the folding of proteins that must remain unfolded until being translocated across membranes. HSP-70 is also abundant in both antimony-resistant *L. braziliensis* and *L. chagasi* lines, suggesting that it is associated with antimony resistance mechanisms and cell development [47]. The Enolase up-regulated in SC6 has been proven to be a virulence factor in *L. mexicana*, *L. donovani,* and *L. major*, and acts as a molecular chaperone [48]. Cyclophilin 40 (CyP40) up-regulated in the JS5 strain is a bifunctional member of the CyP family that not only carries PPIase activity but also plays an important role as cochaperone, forming dynamic complexes with HSP90 in yeast and mammalian cells through a conserved

tetratricopeptide repeat (TPR) domain. *cyp40*-null parasites experience intrinsic homeostatic stress that likely abrogates parasite viability during intracellular infection [49].

The *Leishmania* spp. have developed many strategies to survive and proliferate inside the host cells; some are related to the presence of *Leishmania* surface lipophosphoglycan (LPG) (up-regulated in the JIASHI-5 strain) and glycoprotein 63 (GP63) (up-regulated in the KS-2 and the SC6 strains), and some involve interference with microbial killing by phagocytosis and/or cytokine and chemokine production [50]. The zinc-dependent metalloprotease GP63 or leishmanolysin is a critical virulence factor secreted by *Leishmania*. The *Leishmania donovani* gp63 is necessary for the survival of *Leishmania* in macrophages [51]. Recent studies have suggested that *Leishmania* GP63 is a critical virulence factor in the modulation of many macrophage molecules, and acts to dampen the innate inflammatory responses during early *Leishmania* infection [52]. In this study, prohibitin was most abundant in the JIASHI-5, then in the KS-2 strain. Prohibitin is expressed on the promastigote surface, particularly concentrated at the aflagellar pole and the flagellar pocket. The flagellar pocket is a site of exocytosis and the aflagellar pole is a region of initial contact between the host and the parasite. The macrophage surface HSP70 has been shown as the cognate binding partner for *Leishmania* prohibitin. Jain et al. found that the presence of anti-prohibitin antibodies during macrophage-Leishmania interaction *in vitro* reduces infection, and Leishmania prohibitin can generate a strong humoral response in VL patients [52]. The mitogen-activated protein kinase (MAPK) was most abundant in the KS-2. MAPK is the most downstream kinase in signal transduction cascades and regulates critical cellular activities such as cell proliferation, differentiation, mortality, stress response, and apoptosis. MAPK1 also has kinase activity on substrate HSP90 or HSP70. By phosphorylating HSPs in the foldosome complex, MAPK1 may regulate the stability and activity of the foldosome which in turn plays a pivotal role in the parasitic life cycle of *L. donovani*. Conversely, HSP90 and HSP70 are identified as the first substrates of LdMAPK1.

This study's possible weakness is study do not highlight the information associated with glycoconjugates expressed on the parasite's surface. Analysis including functional assays of glycoconjugates proteins such as gp63 and LPG would have been added information in regards to parasite biology. In conclusion, we used a label-free quantitative proteomic technique to detect protein level differences among three *Leishmania* strains which cause different clinical manifestations of VL. Further proteomic analysis is needed to better understand the infection-associated pathways. The roles of glycoconjugates and infection-associated proteins in the pathogenicity of *Leishmania* infection should be further investigated.

Supplementary Information The online version contains supplementary material available at https://doi.org/10.1007/s11686-021-00387-3.

References

1. Alvar J, Yactayo S, Bern C (2006) Leishmaniasis and poverty. Trends Parasitol 22:552–557. https://doi.org/10.1016/j.pt.2006.09.004
2. Jain S, Rana V, Tridibes A, Sunil S, Bhatnagar RK (2015) Dynamic expression of miRNAs across immature and adult stages of the malaria mosquito *Anopheles stephensi*. Parasit Vectors 8:179. https://doi.org/10.1186/s13071-015-0772-y
3. Guan LR, Shen WX (1991) Recent advances in visceral leishmaniasis in China. Southeast Asian J Trop Med Public Health 22:291–298
4. Bruschi F, Gradoni L (eds) (2018) The leishmaniases: old neglected tropical diseases. Springer, Berlin. https://doi.org/10.21767/1791-809X.1000519
5. Alemayehu B, Alemayehu M (2017) Leishmaniasis: a review on parasite, vector and reservoir host. Health Sci J 11:1. https://doi.org/10.21767/1791-809X.1000519
6. Wong JW, Cagney G (2010) An overview of label-free quantitation methods in proteomics by mass spectrometry. Methods Mol Biol 604:273–283. https://doi.org/10.1007/978-1-60761-444-9_18
7. Zhu W, Smith JW, Huang CM (2010) Mass spectrometry-based label-free quantitative proteomics. J Biomed Biotechnol 2010:840518. https://doi.org/10.1155/2010/840518
8. Megger DA, Bracht T, Meyer HE, Sitek B (2013) Label-free quantification in clinical proteomics. Biochim Biophys Acta 1834:1581–1590. https://doi.org/10.1016/j.bbapap.2013.04.001
9. Etebari K, Hegde S, Saldana MA, Widen SG, Wood TG, Asgari S et al (2017) Global transcriptome analysis of *Aedes aegypti* mosquitoes in response to Zika Virus infection. mSphere 2 2(6):e00456-17. https://doi.org/10.1128/mSphere.00456-17
10. Wang JY, Feng Y, Gao CH, Jin CF, Chen SB, Zhang CJ et al (2007) Asymptomatic Leishmania infection in human population of Wenxian County, Gansu Province. Zhongguo Ji Sheng Chong Xue Yu Ji Sheng Chong Bing Za Zhi 25:62–64
11. Guan LR, Zuo XP, Yimamu (2003) Reemergence of visceral leishmaniasis in Kashi Prefecture, Xinjiang. Zhongguo Ji Sheng Chong Xue Yu Ji Sheng Chong Bing Za Zhi 21:285
12. Guan LR (1991) Current status of kala-azar and vector control in China. Bull World Health Organ 69:595–601
13. Ling L, Kokoza VA, Zhang C, Aksoy E, Raikhel AS (2017) MicroRNA-277 targets insulin-like peptides 7 and 8 to control lipid metabolism and reproduction in *Aedes aegypti* mosquitoes. Proc Natl Acad Sci USA 114:E8017–E8024. https://doi.org/10.1073/pnas.1710970114
14. Cohnstaedt LW, Alfonso-Parra C, Fernandez-Salas I (2017) Mosquito vector biology and control in Latin America-A 27th symposium. J Am Mosq Control Assoc 33:215–224. https://doi.org/10.2987/17-6653.1
15. Wang JY, Cui G, Chen HT, Zhou XN, Gao CH, Yang YT (2012) Current epidemiological profile and features of visceral leishmaniasis in People's Republic of China. Parasit Vectors 5:31. https://doi.org/10.1186/1756-3305-5-31
16. Teixeira PC, Velasquez LG, Lepique AP, de Rezende E, Bonatto JM et al (2015) Regulation of *Leishmania* (L.) amazonensis protein expression by host T cell dependent responses: differential expression of oligopeptidase B, tryparedoxin peroxidase and HSP70 isoforms in amastigotes isolated from BALB/c and BALB/c nude mice. PLoS Negl Trop Dis 9:e0003411. https://doi.org/10.1371/journal.pntd.0003411

17. Zhao G, Qu J, Wang H, Zhong W, Li J, Cui Y, Kong F (2010) Sequence polymorphism analysis of the ITS-1 gene of Leishmania donovani isolates from different epidemic foci in China. Zhongguo Bingyuan Shengwuxue Zazhi/J Pathogen Biol 5:520–523
18. Wisniewski JR, Zougman A, Nagaraj N, Mann M (2009) Universal sample preparation method for proteome analysis. Nat Methods 6:359–362. https://doi.org/10.1038/nmeth.1322
19. Schwanhausser B, Busse D, Li N, Dittmar G, Schuchhardt J, Wolf J et al (2011) Global quantification of mammalian gene expression control. Nature 473:337–342. https://doi.org/10.1038/nature10098
20. Luber CA, Cox J, Lauterbach H, Fancke B, Selbach M, Tschopp J et al (2010) Quantitative proteomics reveals subset-specific viral recognition in dendritic cells. Immunity 32:279–289. https://doi.org/10.1016/j.immuni.2010.01.013
21. Li F, Zhao D, Yang S, Wang J, Liu Q, Jin X et al (2018) ITRAQ-based proteomics analysis of triptolide on human A549 lung adenocarcinoma cells. Cell Physiol Biochem 45:917–934. https://doi.org/10.1159/000487286
22. Wiesgigl M, Clos J (2001) Heat shock protein 90 homeostasis controls stage differentiation in *Leishmania donovani*. Mol Biol Cell 12:3307–3316. https://doi.org/10.1091/mbc.12.11.3307
23. Mishra AK, Agnihotri P, Srivastava VK, Pratap JV (2015) Novel protein-protein interaction between spermidine synthase and *S*-adenosylmethionine decarboxylase from Leishmania donovani. Biochem Biophys Res Commun 456:637–642. https://doi.org/10.1016/j.bbrc.2014.12.008
24. Jiang Y, Roberts SC, Jardim A, Carter NS, Shih S, Ariyanayagam M et al (1999) Ornithine decarboxylase gene deletion mutants of *Leishmania donovani*. J Biol Chem 274:3781–3788. https://doi.org/10.1074/jbc.274.6.3781
25. Kedzierski L, Malby RL, Smith BJ, Perugini MA, Hodder AN, Ilg T et al (2006) Structure of *Leishmania mexicana* phosphomannomutase highlights similarities with human isoforms. J Mol Biol 363:215–227. https://doi.org/10.1016/j.jmb.2006.08.023
26. Mukherjee S, Sen Santara S, Das S, Bose M, Roy J, Adak S (2012) NAD(P)H cytochrome b5 oxidoreductase deficiency in *Leishmania* major results in impaired linoleate synthesis followed by increased oxidative stress and cell death. J Biol Chem 287:34992–35003. https://doi.org/10.1074/jbc.m112.389338
27. Gonzalez D, Perez JL, Serrano ML, Igoillo-Esteve M, Cazzulo JJ, Barrett MP et al (2010) The 6-phosphogluconate dehydrogenase of *Leishmania* (Leishmania) mexicana: gene characterization and protein structure prediction. J Mol Microbiol Biotechnol 19:213–223. https://doi.org/10.1159/000320697
28. Soumya N, Panara MN, Neerupudi KB, Singh S (2017) Functional analysis of an AMP forming acetyl CoA synthetase from *Leishmania donovani* by gene overexpression and targeted gene disruption approaches. Parasitol Int 66:992–1002. https://doi.org/10.1016/j.parint.2016.11.001
29. Kushawaha PK, Gupta R, Sundar S, Sahasrabuddhe AA, Dube A (2011) Elongation factor-2, a Th1 stimulatory protein of *Leishmania donovani*, generates strong IFN-gamma and IL-12 response in cured *Leishmania*-infected patients/hamsters and protects hamsters against *Leishmania* challenge. J Immunol 187:6417–6427. https://doi.org/10.4049/jimmunol.1102081
30. Holmberg L, Nygard O (1994) Interaction sites of ribosome-bound eukaryotic elongation factor 2 in 18S and 28S rRNA. Biochemistry 33:15159–15167. https://doi.org/10.1021/bi00254a027
31. Aoki JI, Muxel SM, Zampieri RA, Laranjeira-Silva MF, Muller KE, Nerland AH et al (2017) RNA-seq transcriptional profiling of *Leishmania amazonensis* reveals an arginase-dependent gene expression regulation. PLoS Negl Trop Dis 11:e0006026. https://doi.org/10.1371/journal.pntd.0006026
32. Rios MC, Silva WR, Azevedo AF, Santos PL, Teixeira SA, Muscara MN et al (2015) Expression of glyceraldehyde 3-phosphate dehydrogenase is enhanced in *Leishmania* spp. naturally resistant to nitric oxide. Genet Mol Res 14:7113–7121. https://doi.org/10.4238/2015.june.29.4
33. Olivier M, Atayde VD, Isnard A, Hassani K, Shio MT (2012) Leishmania virulence factors: focus on the metalloprotease GP63. Microbes Infect 14:1377–1389. https://doi.org/10.1016/j.micinf.2012.05.014
34. Boitz JM, Ullman B (2006) A conditional mutant deficient in hypoxanthine-guanine phosphoribosyltransferase and xanthine phosphoribosyltransferase validates the purine salvage pathway of *Leishmania donovani*. J Biol Chem 2006281:16084–16089. https://doi.org/10.1074/jbc.m600188200
35. Boitz JM, Ullman B (2013) Adenine and adenosine salvage in *Leishmania donovani*. Mol Biochem Parasitol 190:51–55. https://doi.org/10.1016/j.molbiopara.2013.06.005
36. Boitz JM, Strasser R, Yates PA, Jardim A, Ullman B (2013) Adenylosuccinate synthetase and adenylosuccinate lyase deficiencies trigger growth and infectivity deficits in *Leishmania donovani*. J Biol Chem 288:8977–8990. https://doi.org/10.1074/jbc.m112.431486
37. Dey R, Meneses C, Salotra P, Kamhawi S, Nakhasi HL, Duncan R (2010) Characterization of a *Leishmania* stage-specific mitochondrial membrane protein that enhances the activity of cytochrome c oxidase and its role in virulence. Mol Microbiol 77:399–414. https://doi.org/10.1111/j.1365-2958.2010.07214.x
38. Dey R, Dagur PK, Selvapandiyan A, McCoy JP, Salotra P, Duncan R et al (2013) Live attenuated *Leishmania donovani* p27 gene knockout parasites are nonpathogenic and elicit long-term protective immunity in BALB/c mice. J Immunol 190:2138–2149. https://doi.org/10.4049/jimmunol.1202801
39. Van Assche T, Deschacht M, da Luz RA, Maes L, Cos P (2011) Leishmania-macrophage interactions: insights into the redox biology. Free Radic Biol Med 51:337–351. https://doi.org/10.1016/j.freeradbiomed.2011.05.011
40. Suman SS, Amit A, Singh KP, Gupta P, Equbal A, Kumari A et al (2018) Cytosolic tryparedoxin of *Leishmania donovani* modulates host immune response in visceral leishmaniasis. Cytokine 108:1–8. https://doi.org/10.1016/j.cyto.2018.03.010
41. Das S, Giri S, Sundar S, Shaha C (2017) Functional involvement of leishmania donovani tryparedoxin peroxidases during infection and drug treatment. Antimicrob Agents Chemother. https://doi.org/10.1128/aac.00806-17
42. Tessarollo NG, Andrade JM, Moreira DS, Murta SM (2015) Functional analysis of iron superoxide dismutase-A in wild-type and antimony-resistant *Leishmania braziliensis* and *Leishmania infantum* lines. Parasitol Int 64:125–129. https://doi.org/10.1016/j.parint.2014.11.001
43. Gundampati RK, Sahu S, Shukla A, Pandey RK, Patel M, Banik RM et al (2006) Tryparedoxin peroxidase of *Leishmania braziliensis*: homology modeling and inhibitory effects of flavonoids for anti-leishmanial activity. Bioinformation 10:353–357. https://doi.org/10.6026/97320630010353
44. Tellez J, Romero I, Soares MJ, Steindel M, Romanha AJ (2017) Knockdown of host antioxidant defense genes enhances the effect of glucantime on intracellular *Leishmania braziliensis* in human macrophages. Antimicrob Agents Chemother. https://doi.org/10.1128/aac.02099-16
45. Castro H, Sousa C, Santos M, Cordeiro-da-Silva A, Flohe L, Tomas AM (2002) Complementary antioxidant defense by cytoplasmic and mitochondrial peroxiredoxins in *Leishmania infantum*. Free Radic Biol Med 33:1552–1562. https://doi.org/10.1016/s0891-5849(02)01089-4
46. Matrangolo FS, Liarte DB, Andrade LC, de Melo MF, Andrade JM, Ferreira RF et al (2013) Comparative proteomic analysis of antimony-resistant and susceptible *Leishmania braziliensis* and *Leishmania infantum* chagasi lines. Mol Biochem Parasitol 190:63–75. https://doi.org/10.1016/j.molbiopara.2013.06.006

47. Vanegas G, Quinones W, Carrasco-Lopez C, Concepcion JL, Albericio F, Avilan L (2007) Enolase as a plasminogen binding protein in *Leishmania mexicana*. Parasitol Res 101:1511–1516. https://doi.org/10.1007/s00436-007-0668-7
48. Yau WL, Lambertz U, Colineau L, Pescher P, MacDonald A, Zander D et al (2016) Phenotypic characterization of a *Leishmania donovani* cyclophilin 40 null mutant. J Eukaryot Microbiol 63:823–833. https://doi.org/10.1111/jeu.12329
49. Ali KS, Rees RC, Terrell-Nield C, Ali SA (2013) Virulence loss and amastigote transformation failure determine host cell responses to *Leishmania mexicana*. Parasite Immunol 35:441–456. https://doi.org/10.1111/pim.12056
50. Parashar S, Mukhopadhyay A (2017) GTPase Sar1 regulates the trafficking and secretion of the virulence factor gp63 in *Leishmania*. J Biol Chem 292:12111–12125. https://doi.org/10.1074/jbc.m117.784033
51. Hassani K, Shio MT, Martel C, Faubert D, Olivier M (2014) Absence of metalloprotease GP63 alters the protein content of *Leishmania* exosomes. PLoS ONE 9:e95007. https://doi.org/10.1371/journal.pone.0095007
52. Jain R, Ghoshal A, Mandal C, Shaha C (2010) *Leishmania* cell surface prohibitin: role in host-parasite interaction. Cell Microbiol 12:432–452. https://doi.org/10.1111/j.1462-5822.2009.01406.x

Publisher's Note Springer Nature remains neutral with regard to jurisdictional claims in published maps and institutional affiliations.